

SCERPA: a Self-Consistent Algorithm for the Evaluation of the Information Propagation in Molecular Field-Coupled Nanocomputing

*Original*

SCERPA: a Self-Consistent Algorithm for the Evaluation of the Information Propagation in Molecular Field-Coupled Nanocomputing / Ardesi, Yuri; Wang, Ruiyu; Turvani, Giovanna; Piccinini, Gianluca; Graziano, Mariagrazia. - In: IEEE TRANSACTIONS ON COMPUTER-AIDED DESIGN OF INTEGRATED CIRCUITS AND SYSTEMS. - ISSN 0278-0070. - 39:10(2020), pp. 2749-2760. [10.1109/TCAD.2019.2960360]

*Availability:*

This version is available at: 11583/2846076 since: 2021-07-08T11:11:45Z

*Publisher:*

IEEE

*Published*

DOI:10.1109/TCAD.2019.2960360

*Terms of use:*

This article is made available under terms and conditions as specified in the corresponding bibliographic description in the repository

*Publisher copyright*

IEEE postprint/Author's Accepted Manuscript

©2020 IEEE. Personal use of this material is permitted. Permission from IEEE must be obtained for all other uses, in any current or future media, including reprinting/republishing this material for advertising or promotional purposes, creating new collecting works, for resale or lists, or reuse of any copyrighted component of this work in other works.

(Article begins on next page)

# SCERPA: a Self-Consistent Algorithm for the Evaluation of the Information Propagation in Molecular Field-Coupled Nanocomputing

Yuri Ardesi, *Student Member, IEEE*, Ruiyu Wang, Giovanna Turvani, Gianluca Piccinini, Mariagrazia Graziano

**Abstract**—Among the emerging technologies that are intended to outperform the current CMOS technology, the Field-Coupled Nanocomputing (FCN) paradigm is one of the most promising. The Molecular Quantum-dot Cellular Automata (MQCA) has been proposed as possible FCN implementation for the expected very high device density and possible room temperature operations. The digital computation is performed via electrostatic interactions among nearby molecular cells, without the need for charge transport, extremely reducing the power dissipation. Due to the lack of mature analysis and design methods, especially from an electronics standpoint, few attempts have been made to study the behaviour of logic circuits based on real molecules, and this reduces the design capability. In this paper, we propose a novel algorithm, named Self-Consistent Electrostatic Potential Algorithm (SCERPA), dedicated to the analysis of molecular FCN circuits. The algorithm evaluates the interaction among all molecules in the system using an iterative procedure. It exploits two optimizations modes named *Interaction Radius* and *Active Region* which reduce the computational cost of the evaluation, enabling SCERPA to support the simulation of complex molecular FCN circuits and to characterize consequentially the technology potentials. The proposed algorithm fulfils the need for modelling the molecular structures as electronic devices and provides important quantitative results to analyze the information propagation, motivating and supporting further research regarding molecular FCN circuits and eventual prototype fabrication.

**Index Terms**—Field-Coupled Nanocomputing (FCN), Molecular Quantum-dot Cellular Automata (MQCA), Algorithm, Transcharacteristics, Molecular Interaction Modeling.

## I. INTRODUCTION

FIELD-Coupled Nanocomputing (FCN) paradigm uses local field interactions between nanometer-size building blocks to realize logic without the need for charge transport. Several possible implementations have been envisaged for FCN technology [1]–[6], among these, the molecular implementation of the Quantum-dot Cellular Automata (QCA) [7], known as molecular QCA (MQCA) or Molecular FCN, is considered one of the most outstanding solution. The binary information is encoded in the charge configuration of molecules, exploiting redox-active molecular sites as quantum dots [4], [8], [9]. Considering the nanometer size of molecules, room temperature operations are allowed and the density of

Manuscript received July 23, 2019; revised October 3, 2019; accepted November 22, 2019. Date of publication December XX, 2019. Corresponding author: Yuri Ardesi.)

The authors are with the Department of Electronics and Telecommunications, Politecnico di Torino, Torino 10129, Italy (e-mail: yuri.ardesi@polito.it; ruiyu.wang@polito.it; giovanna.turvani@polito.it; gianluca.piccinini@polito.it; mariagrazia.graziano@polito.it).

Digital Object Identifier xx.xxxx/TCAD.xxxx.xxxxxx

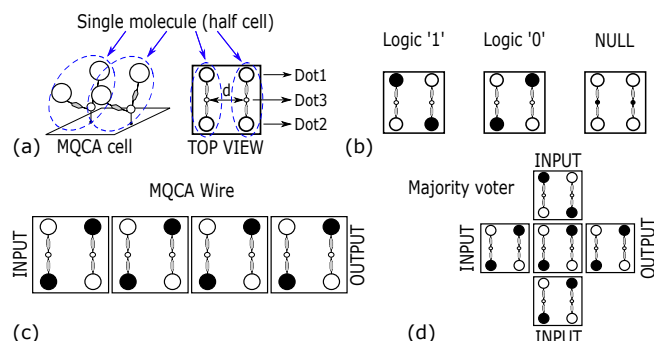


Fig. 1. Basics of MQCA: (a) A complete MQCA cell: two three-dot molecules are juxtaposed to create a squared-shape cell. (b) Stable states of an MQCA cell used for the encoding of the binary information and NULL state. (c) Binary MQCA wire: the binary information is propagated from INPUT cell to the OUTPUT cell, following a domino-like style (d) Majority voter: the three input cells vote on the logic state of the output cell.

devices on the chip is very high [10]. The need for charge transport for the encoding and the elaboration of the information is eliminated and the power dissipation is extremely reduced [11].

The physical properties of single molecules have been deeply analyzed in the literature [9], [12] to show the possibility to achieve digital computation. In this work, we analyze the molecular technology from the electronics perspective by moving the focus from the single-molecule to the system.

Tools such as QCADesigner [13] allows the evaluation of the information propagation in general QCA circuits. The approach considers single cells composed of four charges and employs the two-state quantum mechanics approximation to evaluate the interaction. This approach allows the behavioural simulation of general QCA circuits, yet it hardly fits with the effective electrostatic behaviour of molecules, making the simulation of molecular FCN still challenging. At the current state, there is a lack of mature methods and no available tool to evaluate the molecular interaction, thus the information propagation in FCN circuits, considering the effective molecular physics.

Following the aim of several works such as ToPoliNano [14] and NMLSim [15], allowing the simulation of magnetic FCN technology, and SiQAD [16], simulating the Atomic Silicon Quantum Dot Circuits, we propose a novel algorithm, named SCERPA (Self-Consistent Electrostatic Potential Algorithm), which evaluates the propagation of the information in molecular FCN circuits using an iterative procedure. The

charge distribution of molecules generates electric fields. In a molecular system, each molecule generates an electric field and, in turn, it reacts to the effects induced by other molecule charges. Each state of the system is defined by a charge distribution self-consistent with the induced electric fields.

SCERPA bases the evaluation on the effective electrostatic properties of the molecule, computed through ab initio calculation. The framework allows validating current QCA devices and circuits, designed within the general QCA paradigm, considering the effective physical behaviour of the molecule and the corresponding technological aspects. It allows to quantitatively describe the information propagation in molecular circuits, thus supporting and assessing further research in the field of molecular FCN. It also fulfils our aim to facilitate the design, the analysis and the future fabrication of molecular FCN devices and circuits.

## II. BACKGROUND

### A. The Molecular Field-Coupled Nanocomputing

The basic building block of the molecular technology depicted in Fig. 1(a) is the MQCA cell: two oxidized molecules possessing three redox centres (i.e. atoms which favour the aggregation of the oxidation charge in precise points of the molecule, reported in the figure as *Dot1*, *Dot2* and *Dot3*) are juxtaposed to create a system of six redox centres and two oxidation charges. The MQCA cell is consistent with the general QCA paradigm: an arrangement of six quantum dots and two extra mobile charges.

Following the approach used for general QCA paradigm, three different states are possibly encoded depending on the localization of the two free charges: logic states “0” and “1” are encoded when the two charges occupy the antipodal sites of the cell, as depicted in Fig. 1(b). Instead, when the two charges fill the central dots, the cell encodes the third state (“NULL” state), which does not encode any information but it is essential for realizing the adiabatic switching [17], [18].

Simple logic gates can be implemented by arranging MQCA cells. Fig. 1(c) shows the basic scheme of the binary wire, fundamental for achieving information propagation, whereas Fig. 1(d) shows a majority voter. A possible MQCA inverter is reported in [19]. Based on the mentioned devices, more complex digital devices, such as arithmetic circuits and microprocessors, have been proposed in the literature [20]–[22].

### B. The Bis-Ferrocene molecule

Many molecules have been proposed for the implementation of MQCA technology. The diallyl-butane, the decatriene, and the diferrocenyl carborane have been studied to demonstrate the possibility of achieving FCN computation [4], [9], [23].

In this work, we consider the *bis-ferrocene* molecule, which has been synthesized ad hoc for realizing MQCA and it shows promising potentials for the digital computation [24] [8].

The two ferrocene units act as the logic (or active) dots *Dot1* and *Dot2* used for the logic state encoding. The central carbazole is recognized as *Dot3* and used to encode the “NULL” state. A sulfur-ended alkyl-chain anchors the molecule to the gold substrate by exploiting self-assembly techniques [25].

The atoms of the bis-ferrocene molecule are grouped into functional groups, see Fig. 2(a), constituting the dots required by the general QCA paradigm. A single molecule with three dots constitutes a half MQCA cell; the complete MQCA cell is realized by juxtaposing two molecules, as previously shown in Fig. 1(a). The molecule is considered in the oxidized form as it demonstrates better performance [26]: an electron is removed from the molecule using electrochemistry techniques and its net charge is +1 e. Each molecule is coupled by a counterion which preserves the neutrality of the molecule [8].

To reduce power consumption, the charge in the molecule should be moved slowly to ensure that the molecules lie in the ground state during the switching phase, avoiding abrupt variations in energy of the molecules. This is known as *adiabatic switching* and it is accomplished by exploiting an externally applied electric field named *clock field* [17], [18]. The effects of the field on bis-ferrocene molecules have been characterised in [27]: the molecule free charge can be pushed down to the central *Dot3* (negative clock field), keeping the molecule in “NULL” state, or released to the two logic dots (positive clock field), enabling the switching of the molecule. The application of several negative and positive fields enables the correct adiabatic propagation of data in FCN circuits.

### C. Modeling of the MQCA cell

Fig. 2(c) illustrates a possible implementation of molecular wire. The logic state of the first molecule is fixed by an external stimulus in the logic states “0” or “1”. Molecules that follow modify their charge distribution to minimize the Coulomb repulsion, enabling the information propagation.

Complete ab initio calculations have been used so far to study the single-molecule and the molecule-to-molecule interaction [4], [28], [29], by exploiting point charges for emulating driver molecules (e.g. the input of the molecular

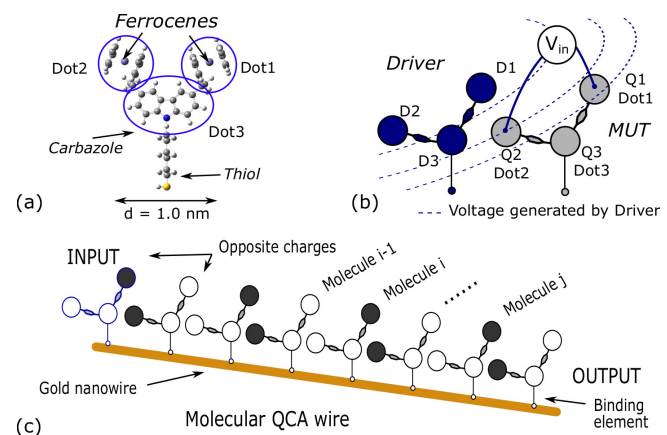


Fig. 2. Modelling of Molecular FCN: (a) Structure of the bis-ferrocene molecule and aggregated charge distribution. (b) Molecule-to-molecule interaction. Driver molecule is emulated by three point charges  $D1$ ,  $D2$  and  $D3$ , depending on charge values, driver logic states 0 and 1 are emulated. The driver influences the *Molecule-Under-Test* (MUT) by generating the *Input-Voltage*  $V_{in}$ . The MUT re-configures its charge distribution modifying the three aggregated charges  $Q1$ ,  $Q2$  and  $Q3$  according to the *Input-Voltage*  $V_{in}$ . (c) Schematic structure of a molecular wire, several bis-ferrocene molecules anchored on a gold nanowire.

wire) [30]. The ab initio calculation is based on the laws of quantum mechanics, thus the analysis of properties is very accurate but very computationally intensive: absolutely unusable for many-molecule devices. In molecular FCN, several components of the local fields are concurrently applied in the circuits to define the state of input driver molecules [31] or to realize the multi-phase clock system necessary to guarantee correct computation and to realize adiabatic switching [18], [32]. The use of point charges in ab initio calculation permits the application of electric fields emulating the presence of external stimuli (e.g. drivers), yet the complexity of the calculation increases, limiting the approach to the analysis of few molecules. These limitations preclude serious analysis of molecular circuits using full ab initio computation, which urgently motivates researchers in seeking an alternative method for the behavioural simulation of devices and circuits.

For instance, general QCA paradigm often makes use of the quantum mechanics two-state approximation (TSA) to model the cell [33]. Authors in [12] provide an accurate analysis of the use of the TSA for the modelling of molecules, demonstrating the possibility of using the TSA for highly-bistable molecules and, more in general, the possibility to use molecules to create MQCA devices. Besides, also the electronic properties of highly bi-stable molecules are well described with the quantum mechanics approximation [9].

Recent studies pointed out the possibility of using monostable molecules as a possible candidate for the molecular FCN paradigm, further reducing the energy dissipation [34], [35].

A different methodology, proposed in [26], characterizes the molecule by using the aggregated charge. Provided the spatial disposition of the molecule, this method gives an accurate description of the molecule electrostatic behaviour and can be applied both to bi-stable and monostable molecules.

#### D. Information propagation in molecular FCN circuits

Despite quantum chemistry is well assessed for the analysis of single-molecules, the simulation of entire circuits using ab initio tools is challenging due to the very high computational cost, absolutely not acceptable for the design purpose.

For this reason, we proposed in [36] an approximated method to describe molecular interactions between consecutive molecules of a wire which performs several ab initio simulations on single molecules and post-processing of data. Firstly, the charge distribution of the first molecule of the wire is evaluated with ab initio simulation. Secondly, the first molecule is substituted with its charge distribution and the second molecule is added. A second ab initio simulation is performed to obtain the charge distribution of the second molecule, under the influence of the first one. The procedure is repeated for all the molecules to obtain the final charge distribution of a wire.

The computational cost of this method is reduced with respect to full ab initio simulation since only single molecules with few point charges are simulated.

This method is trustworthy for an early attempt at describing information propagation along a wire. Nevertheless, it considers the interaction only within two nearby molecules

and evaluates the interaction following the direction of the logic propagation. The method does not take into account that each molecule is able to influence the logic state of any other molecule, independently on their position in the circuit layout. For the general QCA circuits, authors in [33] use an iterative self-consistent procedure to consider this effect. Following, QCADesigner [13] has been developed to analyze general QCA circuits, and more recently enhanced to evaluate the power dissipation [37], [38].

This tool employs the TSA to model the entire QCA cell [39], making the tool very attracting for the simulation of general QCA paradigm. To use QCADesigner in molecular FCN, the user must determine the tunnelling potential ( $\gamma$ ) for the QCA cell via ab initio computation. The cell is composed by two molecules, therefore this value is not a propriety of the single-molecule, yet it depends on geometrical and technological parameters of the cell (e.g. the distance and orientation of molecules in the cell).

In QCAdesigner, the tunnelling potential is the same for all the cells of the circuit: this obstructs the analysis of possible process variation, as it involves variations in the interaction among molecules belonging to different cells. Process variations are instead enabled by molecule-centered models [40].

Correct modelling of molecular technology requires TSA to be applied to the single-molecule [12]. Moreover, the application is limited to simple cases, as more complex molecules require the employment of three states [9].

For these reasons, the TSA model employed in QCADesigner is sufficient to understand the behaviour of general QCA logic which can be potentially implemented with molecular technology, yet it cannot be used to evaluate the effective behaviour of molecular FCN devices. An alternative tool, with molecular granularity, is required to validate circuits considering the effective behaviour, the geometrical and technological characteristics of a molecular cell.

For these reasons, we proposed in [41] a first algorithm for the analysis of devices, enhanced from [36], that considers the interactions among all the molecules without the need for ab initio computation. Each molecule distributes its charge on the dots as a response of the field generated by all the other molecules and, in turn, it generates a field which influences all the other molecules. The procedure is applied to all the molecules of the wire and iterated in a self-consistent way. In [41], a simple wire composed of five molecules was analyzed to demonstrate the possibility of using a self-consistent procedure, based on the aggregated charge, for studying the information propagation in molecular wires. Some studies were also performed with the preliminary algorithm in [40] to analyze the wires on non-ideal substrates.

Taking into account the state-of-the-art, we propose a novel algorithm derived from [41] and named SCERPA, which evaluates the propagation of the information in molecular FCN circuits considering the effective physical properties of the molecule and providing very low computational cost, far lower with respect to ab initio methods.

The proposed algorithm also exploits the characterisation of molecules under electric clock fields [27] to enable the simulation of clocked devices. In this work, we consider the

clock in an optimum condition to favour the intermolecular interaction and, for the sake of clarity, we postpone the discussion and eventual results on clocked devices to future work. We focus the analysis on the information propagation and we evaluate the polarization of each molecule in the circuit, considering the effect of all the possible intermolecular interactions with the aim of facilitating the eventual design, analysis and fabrication of molecular FCN devices.

### III. METHODOLOGY

For the analysis of molecular devices, we use the MosQuiTo (Molecular Simulator Quantum-dot cellular automata Torino) methodology: a three-step methodology (ab initio simulation, post-processing of data, system-level analysis) [26], [30] which describes the molecule as an electronic device, enabling the system-level analysis yet remaining strongly linked to the physics of the molecule. This is a key requirement of nanotechnology devices [42]–[44].

The bis-ferrocene molecule is characterized using ab initio computation (step 1) [30]. The results enable the derivation of figures of merit which model the electrostatic behaviour of the molecule (step 2), enabling the analysis of the intermolecular interaction (step 3) [45].

#### A. Characterization of the molecule through ab initio simulation

To characterize the electrostatic properties of the bis-ferrocene molecule, Density Functional Theory (DFT) is exploited using *Gaussian 09* [46]. Based on the molecular structure of the bis-ferrocene, *B3LYP* and *LANL2DZ* are chosen as suitable functional and basis set [26]. The bis-ferrocene molecule is analyzed considering a positive net charge +1 e to consider the oxidized nature of the molecule.

The characterization of the single-molecule is performed by studying the response of a *Molecule Under Test* (MUT) to the electric field generated by a second molecule, considered as a driver, positioned at a distance  $d$ . The driver molecule is modelled as three aggregated charges which generate an electric field influencing the MUT [27], as shown in Fig. 2(b). The values of the three charges correspond to the aggregated charges (D1, D2, and D3) of the bis-ferrocene molecule computed through DFT analysis under the influence of a positive clock field intended to favour the intermolecular interaction [26]. The clock field forces the oxidation charge to localize in the two logic dots D1 and D2, making almost null the charge in the central dot D3 [27].

The values of D1 and D2 point charges are linearly changed (keeping D1+D2 fixed) until entirely localized on D1 or D2 only to describe all the possible configurations of a driver molecule. With point charge +1.0 e located at D1 or D2, the driver emulates logic states “1” and “0” respectively.

From the DFT results, the aggregated charges are computed summing all the atomic charges obtained by fitting the electrostatic potential following to the *Merz-Singh-Kollman* (MK) approach [47], as shown in Fig. 2(a). This approximation well describes the electrostatic behaviour of the molecule

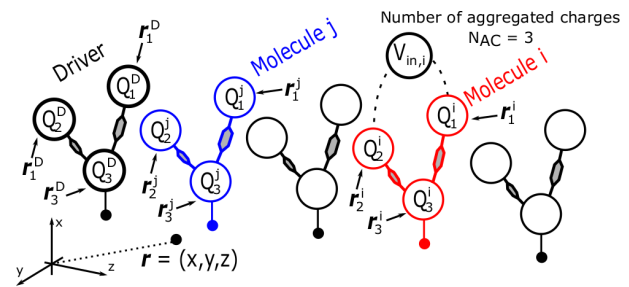


Fig. 3. Schematic model for the intermolecular interaction in SCERPA.

and allows the evaluation of the intermolecular interaction responsible for the FCN computation [26].

To quantitatively compute the intermolecular interaction, the trans-characteristics is evaluated. It links the input voltage  $V_{in}$  to the value of the aggregated charge [26]. The input voltage is obtained by integrating the electric field generated by the driver molecule between the two logical dots ( $Q_1$  and  $Q_2$ ) of the MUT, as depicted in Fig. 2(b). The aggregated charges model the charge distribution of the molecule. The procedure can be repeated by applying different clock fields to obtain clock-dependent transcharacteristics [27].

#### B. Modeling of the electrostatic interaction

Given the aggregated charge of a molecule, the electric field can be computed in any point of the surrounding space through electrostatic equations. For the sake of clarity, we denote the Euclidean distance between two points  $\mathbf{r}_A$  and  $\mathbf{r}_B$  as  $d(\mathbf{r}_A, \mathbf{r}_B)$ .

Assuming that a set of  $N_{AC}$  charges,  $\{Q_1^D, \dots, Q_{N_{AC}}^D\}$  in the positions  $\{\mathbf{r}_1^D, \dots, \mathbf{r}_{N_{AC}}^D\}$ , represents the driver molecule, the voltage generated by the driver  $V_D$  at a generic point in the 3D space  $\mathbf{r}$  can be evaluated as:

$$V_D(\mathbf{r}) = \frac{1}{4\pi\epsilon_0} \sum_{\beta=1}^{N_{AC}} \frac{Q_{\beta}^D}{d(\mathbf{r}_{\beta}^D, \mathbf{r})} \quad (1)$$

Where  $\epsilon_0$  is the vacuum permittivity. Therefore, if  $\mathbf{r}_1^{MUT}$  and  $\mathbf{r}_2^{MUT}$  are the positions of MUT *Dot1* and *Dot2* respectively (active dots), the influence of the driver to the MUT is evaluated as the voltage difference between the two active dot positions:

$$V_{D,MUT} = \int_{\gamma} \mathbf{E}_D \cdot d\mathbf{l} = V_D(\mathbf{r}_1^{MUT}) - V_D(\mathbf{r}_2^{MUT}) \quad (2)$$

Where  $\mathbf{E}_D$  is the electric field generated by driver molecule charge distribution, and  $\gamma$  is a path connecting  $\mathbf{r}_1^{MUT}$  with  $\mathbf{r}_2^{MUT}$ . Notice that the positions of driver molecule and MUT are arbitrarily defined, this allows considering the physical position of the molecules, taking into account possible rotations or misalignment.

Given the input voltage  $V_{D,MUT}$ , the aggregated charges of the bis-ferrocene molecule are obtained by applying the transcharacteristics. This enables the response evaluation of one molecule to the nearby elements, thus the intermolecular interaction.

### C. Modeling of the propagation

The electrostatic interaction among molecules determines the information propagation in the molecular circuit. Based on the unidirectional molecular interaction discussed in [36], we here propose a more comprehensive algorithm for the study of the molecular propagation which considers the interactions among all molecules.

In specific, considering the molecular wire depicted in Fig. 3 as a reference for the analysis, the generic *Molecule j* can be modeled as a set of  $N_{AC}$  charges,  $\{Q_1^j, \dots, Q_{N_{AC}}^j\}$  in the positions  $\{\mathbf{r}_1^j, \dots, \mathbf{r}_{N_{AC}}^j\}$ . The voltage generated by *Molecule j* in a generic  $\mathbf{r}$  point in the 3D space can be evaluated as:

$$V_j(\mathbf{r}) = \frac{1}{4\pi\epsilon_0} \sum_{\beta=1}^{N_{AC}} \frac{Q_\beta^j}{d(\mathbf{r}_\beta^j, \mathbf{r})} \quad (3)$$

*Molecule j* influences all the molecules in the wire, both in the direction of the *INPUT* and the *OUTPUT*. We model a second generic *Molecule i* with the aggregated charges  $\{Q_1^i, \dots, Q_{N_{AC}}^i\}$  in the positions  $\{\mathbf{r}_1^i, \dots, \mathbf{r}_{N_{AC}}^i\}$ . *Molecule j* generates a voltage *Molecule i* evaluated as:

$$\begin{aligned} V_{j,i} &= V_j(\mathbf{r}_1^i) - V_j(\mathbf{r}_2^i) = \\ &= \frac{1}{4\pi\epsilon_0} \sum_{\beta=1}^{N_{AC}} \left[ Q_\beta^j \left( \frac{1}{d(\mathbf{r}_1^i, \mathbf{r}_\beta^j)} - \frac{1}{d(\mathbf{r}_2^i, \mathbf{r}_\beta^j)} \right) \right] \end{aligned} \quad (4)$$

Moreover, once the generic *Molecule i* receives the influence of *Molecule j*, *Molecule i* is considered as a driver that generates its feedback effect back to all the other molecules, *Molecule j* included.

Given the set of  $N$  molecules in the wire, the input voltage  $V_{in,i}$  of *Molecule i* is evaluated by considering the effects of the driver  $V_{D,i}$  and of all the other molecules  $V_{j,i}$ .

Notice that, according to (4),  $V_{j,i}$  depends on the value of *Molecule j* aggregated charges. By introducing the transcharacteristics, the problem is formalized as a non-linear system, as the aggregated charges of *Molecule j* depend on  $V_{in,j}$ . The transcharacteristics is also modulated by the value of the clock which should be applied in the circuit to eventually implement the adiabatic propagation and to guide the information propagation through clock phases.

$$V_{in,i} = V_{D,i} + \sum_{\substack{j=1 \\ j \neq i}}^N V_{j,i}(V_{in,j}, E_{clk,j}) \quad (5)$$

The value of the clock fields  $E_{clk}$  is known a priori and given in input by the user. The algorithm supposes an initial input voltage on all the molecules (i.e.  $\{V_{in,1}^0, \dots, V_{in,N}^0\}$ ), then it iteratively evaluates (5) to determine the approximated solution of the non-linear system in the form:

$$V_{in,i}^k = F_i(V_{in,1}^{k-1}, \dots, V_{in,i-1}^{k-1}, V_{in,i+1}^{k-1}, \dots, V_{in,N}^{k-1}) \quad (6)$$

Where  $k$  represents the single step of the iterative procedure and  $F_i$  denotes the equation (5).

Regarding the convergence of the algorithm, the procedure can be studied as a Fixed-Point method for solving the non-linear system (5). The convergence is ensured when the Jacobian  $J_F$  of function  $F$  satisfies  $\|J_F\| < 1$  for some matrix norm [48]. The Jacobian  $J_F$  is a measure on how much the input voltage of a generic molecule *Molecule i* is affected a possible variation of the generic *Molecule j* input voltage:  $\{J_F\}_{i,j} = \delta V_{in,i} / \delta V_{in,j}$ .

The Jacobian norm mainly depends on the transcharacteristics slope. Indeed, given a precise input voltage, the steeper is the transcharacteristics, the larger is the effect a molecule produces on other molecules.

SCERPA allows the use of a small damping ( $\xi$ ) to improve the convergence of the method: the voltage  $V_{in,i}^k$  in th  $(k+1)$ th step is evaluated as a linear superposition between the value evaluated at the previous step  $V_{in,i}^{k-1}$  and the one which is normally obtained using (6):

$$V_{in,i}^k = \xi V_{in,i}^{k-1} + (1 - \xi) F_i(V_{in,1}^{k-1}, \dots, V_{in,N}^{k-1}) \quad (7)$$

By applying damping, the voltage variation produced by each molecule is damped by a factor  $\xi$  and the Jacobian of the numerical procedure is reduced, improving the convergence of the method. A large damping factor favours the convergence, even though it increases the number of steps required for the convergence of the procedure.

### D. Computational cost reduction

The just-described procedure evaluates the input voltage of  $N$  molecules considering the influence of  $N - 1$  molecules, in each step of the iterative procedure. This procedure becomes computational expensive for circuits composed of many molecules, as the complexity is  $O(N^2)$ . For this reason, two techniques are applied to reduce the number of voltages which are evaluated in each step.

1) *Interaction radius (IR Mode)*: the Coulomb potential is inversely proportional to the distance, therefore the generic *Molecule i* is weakly influenced by far molecules. Instead of evaluating the corresponding  $V_{in,i}$  input voltage by considering the influence of all the molecules in the layout, a maximum distance named *Interaction Radius*  $d_{IR}$  is defined, and only neighbour molecules (IR list) are considered. This technique is also used in [13] for the analysis of general QCA circuits.

Naming  $d$  the intermolecular distance, the number of interactions considered in the evaluation of *Molecule i* input voltage becomes  $2d_{IR}/d$ , thus the total number of evaluated voltages becomes is  $2d_{IR}/d \times N$  and the formal computational cost is  $O(N)$ . Considering the single step, a small Interaction Radius  $d_{IR}$  reduces the number of molecules which are considered for the evaluation, thus decreasing the computational time. A trade-off between computational cost and accuracy is necessary to determine the value of  $d_{IR}$ . In [35] we discussed in details the interaction among molecules in molecular wires considering the interaction on a subset of molecules. In particular, the interaction between one molecule and the neighbours is mainly affected by the interaction with the closest six molecules: a choice of  $d_{IR}$  in the order of six intermolecular distances provides good computational capability and high

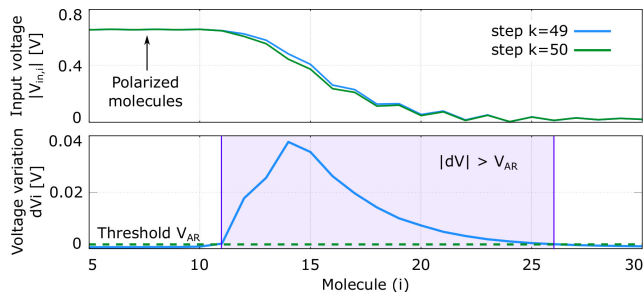


Fig. 4. Voltage  $V_{in,i}$  evaluated in two consecutive steps of a 50 bis-ferrocene wire and corresponding voltage variation  $dV_i = |V_{in,i}^k - V_{in,i}^{k-1}|$ .

precision in the calculation. A large  $d_{IR}$  increases the computational cost, without effectively increasing the precision of the solution. Results regarding the computational cost-accuracy trade-off will be shown in Sec. IV.

2) *Active Region (AR Mode)*: the polarization of molecules is affected by nearby molecules mainly, thus, the molecules which are far from the driver do not vary their charge distribution until nearby molecules become polarized. Consequently, their input voltage is approximately null until the voltage on nearby molecules become relevant. To clarify this point, in Fig. 4 we anticipate the resulting input voltage  $V_{in}$  of a wire composed of 50 molecules, evaluated in two consecutive steps ( $k$ ). The figure shows the absolute value of the input voltage of 25 molecules out of 50 (From *Mol5* to *Mol30*). The figure demonstrates that, once a molecule is polarized, the polarization tends to be constant in the next step. Assuming the possible thermal and electromagnetic noise negligible, only a few input voltages vary appreciably in consecutive steps.

In the Active Region Mode, SCERPA evaluates the voltage of the molecules which are considered active. The variation voltage  $dV_i$  is evaluated in each step as  $|V_{in,i}^k - V_{in,i}^{k-1}|$  and the molecules whose voltage variation is higher than a certain threshold  $V_{AR}$ , with the molecules in their IR list, are set as active (AR list). The Active Region Mode will be motivated further in Section IV. A low value of the threshold  $V_{AR}$  decreases the number of molecules in the AR list, making the single-step calculation rapid. This value should not be chosen too small to avoid an empty AR list.

By applying the AR and IR modes, the formal computational cost of the single-step remains  $O(N)$  as in the worst case all the molecules are active. Nevertheless, the number of molecules in the AR mode is statistically limited to a few molecules, therefore the procedure demonstrates a statistical computational cost which is almost independent on  $N$ .

### E. Implementation

In this work, SCERPA initially supposes a charge distribution on each molecule. Then an iterative procedure is used to determine the approximated solution of the non-linear system and the transcharacteristics is finally applied to obtain the final charge distribution of all the molecules.

The algorithm is subdivided into three parts: initialization stage, interaction stage, output stage.

1) *Initialization Stage*: SCERPA starts with the definition of the biasing conditions and of the geometrical information of the molecular layout: the total number of molecules ( $N$ ), the position of each molecule, and the driver configuration.

SCERPA initially sets the voltage on each molecule equal to zero, then it computes the *Driver Effects*, denoted as  $V_D$ , by evaluating the input voltage generated by the driver cells on each molecule of the circuit (i.e.  $\{V_{D,1}, \dots, V_{D,N}\}$ ).

If the IR or the AR modes are enabled, the algorithm evaluates the IR list of each molecule by calculating all the distances among molecules and comparing them with  $d_{IR}$ .

The driver voltage is used as the first variation voltage  $dV$  to determine the molecules in the AR list. All the molecules satisfying  $V_D > V_{AR}$  and the associated molecules in the IR list are added to the AR list.

2) *Interaction stage*: In this stage, the interaction among molecules is evaluated with an iterative procedure. In the generic  $k$ -th step, all the molecules of the wire influence each other. Precisely, the input voltage of each molecule  $V_{in,i}^k$  is evaluated using (5) and the Voltage Variation is computed as  $dV_i = |V_{in,i}^k - V_{in,i}^{k-1}|$ . Charges used to evaluate  $V_{in,i}^k$  are obtained by using the transcharacteristics.

In this work, we directly evaluate the transcharacteristics using DFT to provide an accurate description of the electrostatic behaviour of the molecule. Alternatively, the molecule can be modelled using the two-state or three-state approximations and the transcharacteristics can be obtained by solving the associated eigenvalue problem [12] [9] [26]. The transcharacteristics is very efficient, as it overcomes the need for solving the eigenvalue problem in the iterative procedure of SCERPA.

To improve the efficiency, all the charges are evaluated on the same set of evenly spaced and ordered voltages  $\{V_{in}^{[1]}, \dots, V_{in}^{[M]}\}$ . Assuming that the generic aggregated charge  $Q_i$  is stored in a vector  $\{Q_i(V_{in}^{[1]}), \dots, Q_i(V_{in}^{[M]})\}$ , the charge can be obtained in a generic  $V_{in}$  by linear approximation:

$$Q_i(V_{in}) = \{w\} \cdot Q_i(\lfloor w \rfloor) + (1 - \{w\}) Q_i(\lfloor w \rfloor + 1) \quad (8)$$

Where  $\{\cdot\}$  and  $\lfloor \cdot \rfloor$  represent the fractional part and the floor functions respectively.  $w$  is the probe position, which is evaluated as:

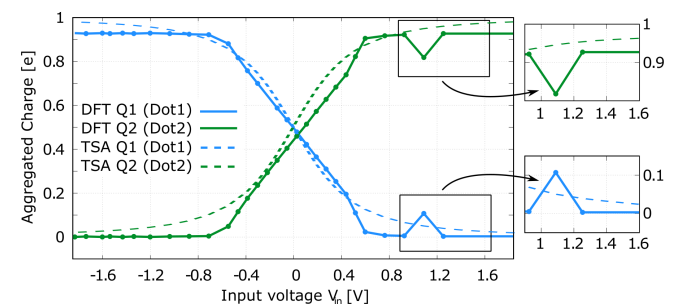


Fig. 5. Transcharacteristics of an oxidized bis-ferrocene molecule in presence of a positive clock signal, values of logical dots (Dot1 and Dot2) obtained by the post-processing of ab initio data.



TABLE I  
CELL-TO-CELL POLARIZATION RESPONSE

Intermolecular distance	Input Polarization	Output Polarization		
		ab initio	SCERPA	QCADesigner
1 nm	+1	+0.385	+0.470	+0.488
1 nm	-1	-0.369	-0.5015	-0.488
0.8 nm	+1	+0.801	+0.8923	+0.575
0.8 nm	-1	-0.823	-0.810	-0.575

TABLE II  
CELL-TO-CELL RESPONSE

	Dr_cell		Ab initio		SCERPA		TSA*	
	D1	D2	Mol1	Mol2	Mol1	Mol2	Mol1	Mol2
Dot1 [e]	1	0	0.782	0.403	0.798	0.336	0.853	0.287
Dot2 [e]	0	1	0.186	0.587	0.134	0.603	0.147	0.713
Dot3 [e]	0	0	0.032	0.010	0.068	0.063	-	-

(\*) Computed with SCERPA by using the transcharacteristics obtained with the Two-State Approximation.

### B. Analysis of the cell-to-cell interaction

The cell-to-cell interaction has been evaluated in SCERPA and validated by comparing the obtained results with the ones from ab initio calculation.

A driver cell (*Dr\_cell*) is set with both logic states and a complete MQCA cell (*Mol1* and *Mol2*) is positioned close to the driver. Fig. 6 shows the obtained results. The circle diameters in the figure represent the aggregated charge value.

Two intermolecular distances are considered: 1 nm and 0.8 nm. In the first case, the two molecules correctly distribute the aggregated dot charges to comply with the logic state of the driver cell. The MQCA cell has a bi-stable cell-to-cell response with respect to the driver cell, see Fig. 6(a) and Fig. 6(b). With the shortest intermolecular distance, the stronger electrostatic repulsion enhances the intermolecular interaction. In this case, the charge separation between logic dots is larger than the 1 nm case, see Fig. 6(c) and Fig. 6(d).

For the sake of completeness, the cell-to-cell interaction is evaluated also using QCADesigner, the tunnelling potential is obtained for a cell composed by two molecules with 1 nm intermolecular distance ( $\gamma = 4.27 \times 10^{-20}$  J). Table I reports

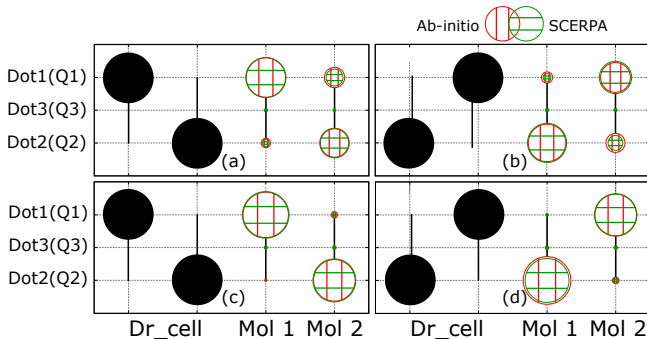


Fig. 6. Comparison in the aggregated charges obtained with SCERPA and DFT for a complete MQCA cell with different driver configurations and intermolecular distances: (a) Logic 1,  $d = 1.0$  nm; (b) Logic 0,  $d = 1.0$  nm; (c) Logic 1,  $d = 0.8$  nm; (d) Logic 0,  $d = 0.8$  nm.

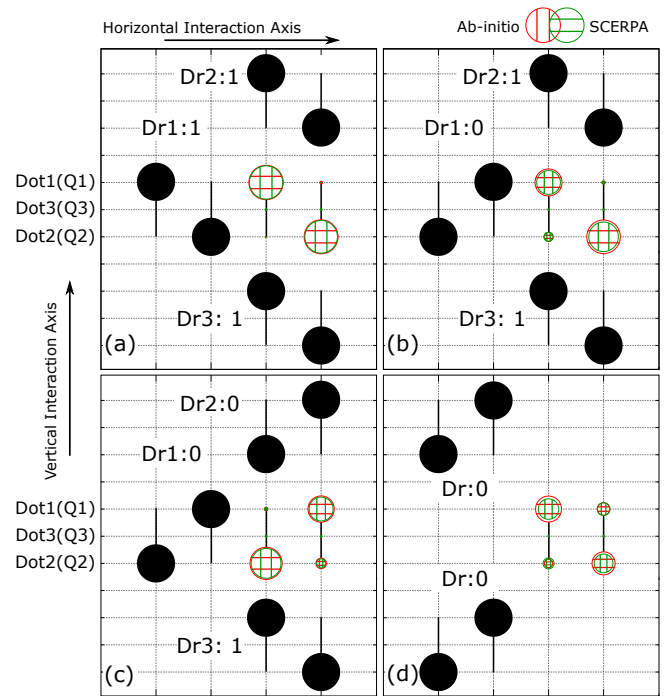


Fig. 7. Comparison in the aggregated charges obtained with SCERPA and DFT for two-dimensional devices in key configurations: (a) Majority voter with all drivers imposing “Logic 1”, the output is “Logic 1”. (b) Majority voter with one driver (Dr1) imposing “Logic 0” and two drivers (Dr2 and Dr3) imposing “Logic 1”, the output is “Logic 1”. (c) Majority voter with two drivers (Dr1 and Dr2) imposing “Logic 0” and one driver (Dr1) imposing “Logic 1”, the output is “Logic 0”. (d) Basic inverter with two drivers imposing “Logic 0”, the output is “Logic 1”.

the results in terms of cell polarization ( $P$ ): the quantity used by QCADesigner and evaluated for SCERPA as

$$P = \frac{Q_{1,Mol1} + Q_{2,Mol2} - Q_{2,Mol1} - Q_{1,Mol2}}{Q_{1,Mol1} + Q_{2,Mol2} + Q_{2,Mol1} + Q_{1,Mol2}} \quad (10)$$

Where the four charges  $Q_i$  are depicted in Fig. 6. As already stated in Sec. II, this parameter depends on the intermolecular interaction. The QCADesigner simulation well matches with the cell-to-cell interaction obtained with DFT and SCERPA for the 1 nm case, yet the precision decrease when the intermolecular distance is reduced to 0.8 nm, a direct consequence of the non-technological granularity of the simulation. On the contrary, the molecular granularity of SCERPA lead to good results also with different intermolecular distance and, more in general enables the study of process variation.

Table II reports the values obtained by SCERPA with “Logic 0” input and 1.0 nm as intermolecular distance. For the sake of completeness, the cell-to-cell interaction evaluated also by modelling the single molecule with a transcharacteristics obtained from a two-state approximation.

### C. Analysis of 2D interaction

To validate SCERPA on more elaborate circuits, we analyse the majority voter and the inverter. The implementation of complete devices requires the definition of clock phases which are out of the scope of this work and will be addressed

in a dedicate paper. We limit the analysis to the study of the key interaction between the input and output cells to validate SCERPA on possible devices involving intermolecular interaction on both the horizontal and vertical interaction axes.

The horizontal intermolecular distance is kept to 1 nm whereas, considering the size of the molecule, the vertical intermolecular distance is set to 2 nm to match the distance between active dots and horizontal intermolecular distance.

Driver cells are modelled by point charges to force fixed logic values. All the possible logic configurations are analysed using both DFT and SCERPA. Fig. 7 shows the results.

When the driver cells impose in the majority voter all the same input, Fig. 7(a), the output follows the input. Same holds when a single input is changed, Fig. 7(b), since the most recurrent input remains the same. When two out of three inputs are changed, the most recurrent input is changed and the output follows the new most recurrent value, as shown in Fig. 7(c). Finally, Fig. 7(d) shows a basic example of an inverter. In this case, the two drivers emulate the presence of an input which is copied on two parallel branches. The electrostatic repulsion forces the output logic to be inverted with respect to the one encoded by the two drivers.

For both the majority voter and the inverter, not reported configurations (i.e. not shown in Fig. 7) are electrostatically equivalent to those shown and are not reported for the sake of brevity. In all the analysed cases, the obtained outputs are consistent with the associated expected behaviour, validating the functioning of the two devices [19]. Also, the results provided by SCERPA well approximate DFT analysis, further confirming the consistency of the proposed algorithm with respect to ab initio methods.

#### D. Analysis of the molecular wire propagation

To demonstrate the functionality of the proposed algorithm, a molecular wire of 40 bis-ferrocene molecules is analyzed.

Fig. 8 shows the electric potential generated by the charge distributions of molecules which have been obtained with SCERPA in different simulation steps. In the first step ( $k=1$ ), shown in Fig. 8(a), the algorithm evaluates the driver contribution  $V_D$  for all the molecules. The driver impacts on the first molecule of the wire, slightly varying the polarization of the next ones. Fig. 8(b) and Fig. 8(c) show two steps ( $k=75$  and  $k=150$ ) of the iterative procedure, a propagation front shows up during the propagation of the information. It can be clearly seen that, considering the two different steps, the polarization of the molecules which are not within the two propagation fronts is constant. This effect motivates the use of the AR mode. Once the algorithm converges, the final wire charge distribution demonstrates the correct propagation of the information, see Fig. 8(d), propagating the Logic 0 to the last two molecules of the wire.

#### E. Information propagation in bis-ferrocene and decatriene molecular wires

SCERPA analyze any molecule provided its transcharacteristics and the proper aggregated charge definition. As a possible application, we analyze two cases of molecular wires made with eight bis-ferrocene and decatriene molecules respectively.

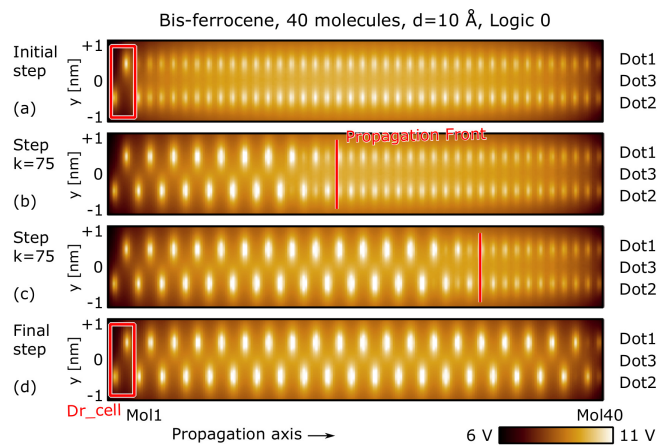


Fig. 8. Propagation in a 40 molecule bis-ferrocene wire evaluated in different steps of SCERPA, electric potential distribution computed at 0.2 nm above the active dot plane. Intermolecular distance is fixed to 1.0 nm: (a) step 1 (driver contribution), (b) step 75 (c) step 150 (d) final result.

Fig. 9 shows the electric potential generated by the charge distributions of bis-ferrocene molecules obtained with SCERPA. With the 1.0 intermolecular distance, each molecule explicitly encodes the correct logic state, properly propagating the binary information. It is worth highlighting that a reduction of the charge separation for the last molecules is present. This is a border effect: molecules in the centre of the wire strongly interact with the two adjacent molecules, enhancing the bi-stability of the molecule thus the charge separation in logic dots. The last molecule has only one neighbour molecule, therefore the input voltage is lower and the charge separation is reduced [35]. This effect has been predicted also for general QCA wires [33]. With intermolecular distance set to 0.8 nm, the stronger intermolecular interaction reduces the border effect, leading to a clearer information propagation.

We analyze, as a second example, the information propagation in wires assembled with the decatriene molecule. For this molecule, we use the transcharacteristics reported in [26].

We set the intermolecular distance equal to the molecule width (0.56 nm) to create an ideal square-shaped MQCA

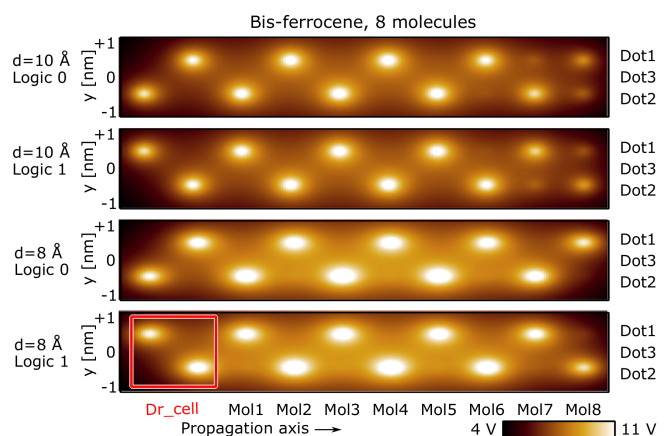


Fig. 9. Propagation of binary information in a 8 molecule bis-ferrocene wire with intermolecular distances 1 nm and 0.8 nm, electric potential distribution evaluated at 0.2 nm above the active dot plane.

cell and we evaluate the propagation of the information with SCERPA. Fig. 10 shows the obtained results. With the considered intermolecular distance, the molecule does not show promising results as the information does not propagate correctly. This result points out the need for a stronger electrostatic interaction in decatriene wires.

With a 0.3 nm intermolecular distance, the decatriene wire shows correct information propagation. The possible difficulties in the realization of a wire with very short intermolecular distances are out of the scope of this work and have been discussed in the [40]. This analysis demonstrates the ability of SCERPA to study the effects at the system level of technological parameters.

### F. Analysis of clocked bis-ferrocene molecular wires

SCERPA also analyzes clocked molecular devices. As already stated, a complete discussion about clocked devices requires deep discussion and will be presented in future work.

To demonstrate the SCERPA functionality and flexibility, we report the simplest case of a wire made with eighteen bis-ferrocene molecules subdivided into three clock regions (6 molecules each clock region). Clock regions can be activated with a positive electric field: the charge distributes on the logic dots according to the transcharacteristics shown in Fig. 5. Alternatively, clock regions can be inhibited with a negative electric field which forces the charge to completely aggregate in *Dot3*, see Fig. 1, minimizing the intermolecular interaction.

Fig. 11 shows the electric potential generated by the molecules computed with SCERPA in three different snapshots. Firstly (T0), only the first region is activated, the first six molecules correctly propagate the information of the driver. Secondly (T1), also the second clock region is activated. The information propagates from the first to the second region. The third clock region is activated only in the third snapshot (T3). Here, the first clock region is inhibited and the information is erased. The second clock region acts as a driver for the third clock region, allowing the information to propagate to the wire end.

### G. Analysis of the computational cost

To analyze the computational cost of SCERPA and the different optimization techniques discussed in Section III, wires made up with different numbers of bis-ferrocene molecules ( $N$ ) are studied using MATLAB. Fig. 12 shows the analysis performed for the three operating modes discussed below.

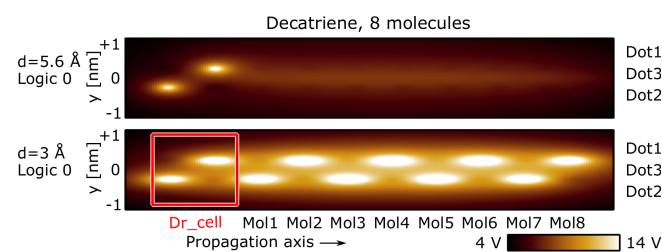


Fig. 10. Propagation of binary information in a 8 molecule decatriene wire with intermolecular distances 0.56 nm and 0.3 nm, electric potential distribution evaluated at 0.1 nm above the active dot plane.

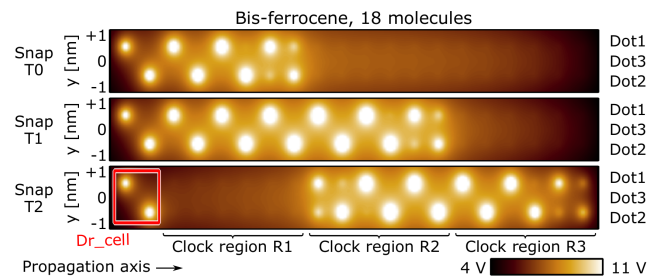


Fig. 11. Three different snapshots (T0, T1, and T2) of the information propagation in a clocked wire composed by 18 bis-ferrocene molecules and subdivided into three clock regions (R1, R2, and R3). Electric potential distribution evaluated at 0.2 nm above the active dot plane. In T0, R1 is activated, R2 and R3 are inhibited. In T1, R1 and R2 are activated, R3 is inhibited. In T2, R2 and R3 are activated, R1 is inhibited.

In MODE I, SCERPA evaluates in each step the input voltage of all  $N$  molecules considering the contributions of other  $N-1$  molecules. As stated in Section III, the formal cost of the single step is  $O(N^2)$ . By considering the self-consistent loop, the effective cost of the total algorithm becomes close to  $O(N^3)$ . The analysis of 500 molecules requires more than 17 hours (on Intel Xeon E3-12, 2 GHz, single-core).

In MODE II, AR and IR modes are enabled. The AR mode is automatically disabled when the AR list becomes empty. As mentioned in Section III, the single-step cost should be statistically independent of  $N$ . This is confirmed by analyzing the average time for the evaluation of a single step ( $t_s$ ), reported in Fig. 12. The 500 molecule wire is evaluated in 128 s and the cost of the total procedure becomes close to the  $O(N)$ . The error  $\sigma$  introduced by the AR and IR modes is evaluated as the relative error of  $|V_{in}|$ , obtained with MODE II, with respect to the voltage obtained using MODE I:

$$\sigma = \frac{|V_{in} - V_{in,MODE I}|}{|V_{in,MODE I}|} \quad (11)$$

The analysis reported in Fig. 12 shows that the AR and IR modes introduce a negligible error in the final result ( $< 1\%$ ).

MODE III represents an intermediate evaluation between MODE I and MODE II: SCERPA initially computes the interaction using MODE II. Then, MODE I is activated (i.e. AR and IR modes are disabled) when it reaches the convergence in order to refine the solution. In MODE III, the error is eliminated (i.e. the result is the same of MODE I). Clearly,

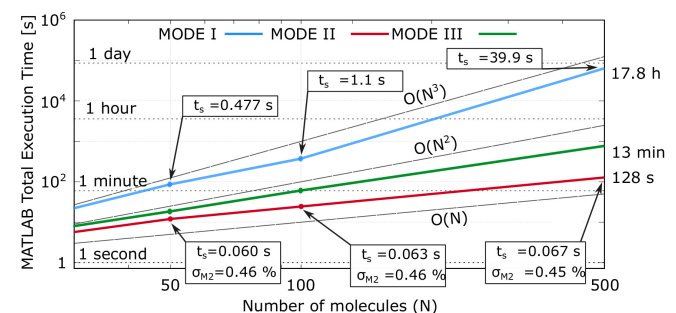


Fig. 12. Computational analysis of SCERPA using all calculation modes. Data obtained with MATLAB on Intel Xeon E3-12 single core (2.00 GHz).

MODE III increases the computational time, that is in any case far lower than the one of MODE I, as shown in Fig. 12.

Finally, a wire composed of 100 molecules is simulated by activating the IR mode only and varying  $d_{IR}$ . With  $d_{IR} = 6$  nm, the time step ( $t_s$ ) is 120 ms and the relative error, evaluated with (11),  $\sigma = 0.005$ . As expected, the computational cost linearly increase with the interaction radius ( $t_s$  is 162 ms and 198 ms for  $d_{IR} = 8$  nm, and 10 nm, respectively) whereas it decreases for smaller interaction radius ( $t_s = 84$  ms for  $d_{IR} = 4$  nm). Concerning the error, it promptly increases for small interaction radius ( $\sigma = 0.015$  for  $d_{IR} = 4$  nm) whereas it becomes negligible for larger  $d_{IR}$  ( $t_s$  is 0.002 and 0.001 for  $d_{IR} = 8$  nm, and 10 nm, respectively).

## V. CONCLUSION

Following the aim of studying the information propagation in molecular FCN circuits from an electronic point of view, an effective algorithm named Self-Consistent ElectRostatic Potential Algorithm (SCERPA) has been proposed.

The single molecule is characterized by evaluating the transcharacteristics, i.e. the correlation between the aggregated charges and the input voltage, using ab initio computation. The transcharacteristics well describe the behaviour of the considered molecules and enable the calculation of the charge distribution of the circuit by evaluating the electrostatic interaction among molecules.

Ab initio calculation is used only to derive the transcharacteristics of the molecule, whereas the intermolecular interaction and the information propagation are evaluated by using electrostatic equations, providing low computational cost and maintaining good precision. The cell-to-cell interaction, the majority voter and the inverter are evaluated using SCERPA and compared to ab initio calculation results. The agreement among values gives a proof of the validity of the proposed algorithm which demonstrates to be functional.

Several molecular wires are analyzed: the algorithm evaluates the propagation of the digital information and highlights the charge separation in all molecules of the wire.

We develop two optimization modes named *Interaction Radius* and *Active Region* which decrease the computational cost of the algorithm, allowing SCERPA to evaluate the polarization of hundreds of molecules in a very small time. In a wire composed of 500 molecules, the evaluation time has been reduced from 17.8 hours to 128 seconds. The error introduced by the two modes is very low (0.45 %).

SCERPA allows comparing the effects of molecular and technological parameters: molecular transcharacteristics, intermolecular distance, rotation, misalignment, vacancies and fabrication defects. The algorithm is general and can be used to analyze complex molecular FCN devices and circuits made with future molecules, provided their transcharacteristics.

The proposed algorithm contributes to the definition of a framework for the design and the analysis of molecular FCN circuits from an electronics perspective. Important feedback between circuit designers and technologists can be provided to facilitate the future fabrication of a molecular FCN prototype.

## REFERENCES

- [1] C. S. Lent and P. D. Tougaw, "Bistable saturation due to single electron charging in rings of tunnel junctions," *Journal of Applied Physics*, vol. 75, no. 8, pp. 4077–4080, 1994.
- [2] Orlov, Imre, Csaba, Ji, Bernstein, and G. H., "Magnetic quantum-dot cellular automata: Recent developments and prospects," Mar 2008.
- [3] M. Vacca, F. Cairo, G. Turvani, F. Riente, M. Zamboni, and M. Graziano, "Virtual clocking for nanomagnet logic," *IEEE Transactions on Nanotechnology*, vol. 15, pp. 962–970, Nov 2016.
- [4] C. S. Lent, B. Isaksen, and M. Lieberman, "Molecular quantum-dot cellular automata," *Journal of the American Chemical Society*, vol. 125, no. 4, pp. 1056–1063, 2003. PMID: 12537505.
- [5] A. Chiolerio, P. Allia, and M. Graziano, "Magnetic dipolar coupling and collective effects for binary information codification in cost-effective logic devices," *Journal of Magnetism and Magnetic Materials*, vol. 324, no. 19, pp. 3006 – 3012, 2012.
- [6] M. Vacca, J. Wang, M. Graziano, M. R. Roch, and M. Zamboni, "Feedbacks in qca: A quantitative approach," *IEEE Transactions on Very Large Scale Integration (VLSI) Systems*, vol. 23, pp. 2233–2243, Oct 2015.
- [7] C. S. Lent, P. D. Tougaw, W. Porod, and G. H. Bernstein, "Quantum cellular automata," *Nanotechnology*, vol. 4, no. 1, p. 49, 1993.
- [8] V. Arima, M. Iurlo, L. Zoli, S. Kumar, M. Piacenza, F. Della Sala, F. Matino, G. Maruccio, R. Rinaldi, F. Paolucci, M. Marcaccio, P. G. Cozzi, and A. P. Bramanti, "Toward quantum-dot cellular automata units: thiolated-carbazole linked bisferrocenes," *Nanoscale*, vol. 4, no. 3, pp. 813–823, 2012.
- [9] Y. Lu, M. Liu, and C. Lent, "Molecular quantum-dot cellular automata: From molecular structure to circuit dynamics," *Journal of Applied Physics*, vol. 102, no. 3, p. 034311, 2007.
- [10] C. S. Lent, "Bypassing the transistor paradigm," *Science*, vol. 288, no. 5471, pp. 1597–1599, 2000.
- [11] J. Timler and C. S. Lent, "Power gain and dissipation in quantum-dot cellular automata," *Journal of Applied Physics*, vol. 91, no. 2, pp. 823–831, 2002.
- [12] Y. Lu and C. S. Lent, "A metric for characterizing the bistability of molecular quantum-dot cellular automata," *Nanotechnology*, vol. 19, p. 155703, mar 2008.
- [13] K. Walus, T. J. Dysart, G. A. Jullien, and R. A. Budiman, "Qcadesigner: a rapid design and simulation tool for quantum-dot cellular automata," *IEEE Transactions on Nanotechnology*, vol. 3, pp. 26–31, March 2004.
- [14] F. Riente, G. Turvani, M. Vacca, M. R. Roch, M. Zamboni, and M. Graziano, "Topolinano: A cad tool for nano magnetic logic," *IEEE Transactions on Computer-Aided Design of Integrated Circuits and Systems*, vol. 36, pp. 1061–1074, July 2017.
- [15] T. R. B. S. Soares, J. G. Nizer Rahmeier, V. C. de Lima, L. Lascasas, L. G. Costa Melo, and O. P. Vilela Neto, "Nmlsim: a nanomagnetic logic (nml) circuit designer and simulation tool," *Journal of Computational Electronics*, vol. 17, pp. 1370–1381, Sep 2018.
- [16] S. Ng, J. Retallick, H. N. Chiu, R. Lupoiu, M. Rashidi, W. Vine, T. Dienel, L. Livadaru, R. A. Wolkow, and K. Walus, "Siqad: A design and simulation tool for atomic silicon quantum dot circuits," 2018.
- [17] G. Tóth and C. S. Lent, "Quasiadiabatic switching for metal-island quantum-dot cellular automata," *Journal of Applied Physics*, vol. 85, no. 5, pp. 2977–2984, 1999.
- [18] V. Vankamamidi, M. Ottavi, and F. Lombardi, "Two-dimensional schemes for clocking/timing of qca circuits," *IEEE Transactions on Computer-Aided Design of Integrated Circuits and Systems*, vol. 27, pp. 34–44, Jan 2008.
- [19] M. Ottavi, S. Pontarelli, E. P. DeBenedictis, A. Salsano, S. Frost-Murphy, P. M. Kogge, and F. Lombardi, "Partially reversible pipelined qca circuits: Combining low power with high throughput," *IEEE Transactions on Nanotechnology*, vol. 10, pp. 1383–1393, Nov 2011.
- [20] M. Awais, M. Vacca, M. Graziano, and G. Masera, "Fft implementation using qca," in *2012 19th IEEE International Conference on Electronics, Circuits, and Systems (ICECS 2012)*, pp. 741–744, Dec 2012.
- [21] M. Awais, M. Vacca, M. Graziano, M. R. Roch, and G. Masera, "Quantum dot cellular automata check node implementation for ldpc decoders," *IEEE Transactions on Nanotechnology*, vol. 12, pp. 368–377, May 2013.
- [22] P. D. Tougaw and C. S. Lent, "Logical devices implemented using quantum cellular automata," *Journal of Applied Physics*, vol. 75, no. 3, pp. 1818–1825, 1994.
- [23] J. A. Christie, R. P. Forrest, S. A. Corcelli, N. A. Wasio, R. C. Quardokus, R. Brown, S. A. Kandel, Y. Lu, C. S. Lent, and K. W. Henderson, "Synthesis of a neutral mixed-valence diferrocenyl carborane

- for molecular quantum-dot cellular automata applications,” *Angewandte Chemie International Edition*, vol. 54, no. 51, pp. 15448–15451, 2015.
- [24] L. Zoli, *Active bis-ferrocene molecules as unit for molecular computation*. PhD thesis, Università di Bologna, Bologna, Italy, 2010.
- [25] A. Pulimeno, M. Graziano, A. Sanginario, V. Cauda, D. Demarchi, and G. Piccinini, “Bis-ferrocene molecular qca wire: Ab initio simulations of fabrication driven fault tolerance,” *IEEE Transactions on Nanotechnology*, vol. 12, pp. 498–507, July 2013.
- [26] Y. Ardesi, A. Pulimeno, M. Graziano, F. Riente, and G. Piccinini, “Effectiveness of molecules for quantum cellular automata as computing devices,” *Journal of Low Power Electronics and Applications*, vol. 8, no. 3, 2018.
- [27] R. Wang, A. Pulimeno, M. R. Roch, G. Turvani, G. Piccinini, and M. Graziano, “Effect of a clock system on bis-ferrocene molecular qca,” *IEEE Transactions on Nanotechnology*, vol. 15, pp. 574–582, July 2016.
- [28] C. S. Lent and B. Isaksen, “Clocked molecular quantum-dot cellular automata,” *IEEE Transactions on Electron Devices*, vol. 50, pp. 1890–1896, Sep. 2003.
- [29] A. M. Pintus, A. Gabrieli, F. G. Pazzona, G. Pireddu, and P. Demontis, “Molecular qca embedding in microporous materials,” *Phys. Chem. Chem. Phys.*, pp. –, 2019.
- [30] A. Pulimeno, M. Graziano, A. Antidormi, R. Wang, A. Zahir, and G. Piccinini, *Understanding a Bisferrocene Molecular QCA Wire*, pp. 307–338. Berlin, Heidelberg: Springer Berlin Heidelberg, 2014.
- [31] A. Pulimeno, M. Graziano, D. Demarchi, and G. Piccinini, “Towards a molecular qca wire: simulation of write-in and read-out systems,” *Solid-State Electronics*, vol. 77, pp. 101 – 107, 2012. Special Issue of IEEE INEC 2011 (IEEE International Nano Electronics Conference).
- [32] M. Graziano, M. Vacca, A. Chiolerio, and M. Zamboni, “An ncl-hdl snake-clock-based magnetic qca architecture,” *IEEE Transactions on Nanotechnology*, vol. 10, pp. 1141–1149, Sep. 2011.
- [33] C. S. Lent and P. D. Tougaw, “Lines of interacting quantum-dot cells: A binary wire,” *Journal of Applied Physics*, vol. 74, no. 10, pp. 6227–6233, 1993.
- [34] E. Rahimi and J. R. Reimers, “Molecular quantum cellular automata cell design trade-offs: latching vs. power dissipation,” *Phys. Chem. Chem. Phys.*, vol. 20, pp. 17881–17888, 2018.
- [35] Y. Ardesi, L. Gnoli, M. Graziano, and G. Piccinini, “Bistable propagation of monostable molecules in molecular field-coupled nanocomputing,” in *2019 15th Conference on Ph.D Research in Microelectronics and Electronics (PRIME)*, pp. 225–228, July 2019.
- [36] A. Pulimeno, M. Graziano, R. Wang, D. Demarchi, and G. Piccinini, “Charge distribution in a molecular qca wire based on bis-ferrocene molecules,” in *2013 IEEE/ACM International Symposium on Nanoscale Architectures (NANOARCH)*, pp. 42–43, July 2013.
- [37] S. Srivastava, A. Asthana, S. Bhanja, and S. Sarkar, “Qcapro - an error-power estimation tool for qca circuit design,” in *2011 IEEE International Symposium of Circuits and Systems (ISCAS)*, pp. 2377–2380, May 2011.
- [38] F. Sill Torres, R. Wille, P. Niemann, and R. Drechsler, “An energy-aware model for the logic synthesis of quantum-dot cellular automata,” *IEEE Transactions on Computer-Aided Design of Integrated Circuits and Systems*, vol. 37, pp. 3031–3041, Dec 2018.
- [39] G. Toth, *Correlation and Coherence in Quantum-Dot Cellular Automata*. PhD thesis, Univ. Notre Dame, Notre Dame, IN, USA, 2000.
- [40] M. Graziano, R. Wang, M. R. Roch, Y. Ardesi, F. Riente, and G. Piccinini, “Characterisation of a bis-ferrocene molecular qca wire on a non-ideal gold surface,” *Micro Nano Letters*, vol. 14, no. 1, pp. 22–27, 2019.
- [41] R. Wang, M. Chilla, A. Palucci, M. Graziano, and G. Piccinini, “An effective algorithm for clocked field-coupled nanocomputing paradigm,” in *2016 IEEE Nanotechnology Materials and Devices Conference (NMDC)*, pp. 1–2, Oct 2016.
- [42] M. Vacca, G. Turvani, F. Riente, M. Graziano, D. Demarchi, and G. Piccinini, “Tamtams: An open tool to understand nanoelectronics,” in *Nanotechnology (IEEE-NANO), 2012 12th IEEE Conference on*, pp. 1–5, Aug 2012.
- [43] G. Turvani, F. Riente, M. Graziano, and M. Zamboni, “A quantitative approach to testing in quantum dot cellular automata: Nanomagnet logic
- case,” in *Ph.D. Research in Microelectronics and Electronics (PRIME), 2014 10th Conference on*, pp. 1–4, June 2014.
- [44] G. Causapruno, F. Riente, G. Turvani, M. Vacca, M. R. Roch, M. Zamboni, and M. Graziano, “Reconfigurable systolic array: From architecture to physical design for nml,” *IEEE Transactions on Very Large Scale Integration (VLSI) Systems*, vol. 24, no. 11, pp. 3208 – 3217, 2016.
- [46] M.J. Frisch et al, “Gaussian09 revision a.1,” 2009. Gaussian Inc.Wallingford CT.
- [47] U. C. Singh and P. A. Kollman, “An approach to computing electrostatic charges for molecules,” *Journal of Computational Chemistry*, vol. 5, no. 2, pp. 129–145, 1984.
- [48] A. Quarteroni, R. Sacco, and F. Saleri, *Numerical Mathematics (Texts in Applied Mathematics)*. Berlin, Heidelberg: Springer-Verlag, 2006.
- Yuri Ardesi** received the M.Sc. degree in Electronics Engineering in 2017 from Politecnico di Torino, where he is currently pursuing the Ph.D. degree. His research interests include molecular Field-Coupled Nanocomputing and nanotechnology.
- Ruiyu Wang** received the M.Sc. degree in Electronics Engineering from Politecnico di Torino, in 2013, and the Ph.D. degree in electronics and communication engineering in 2017. His research interests include the analysis and the architectural modulation of molecular quantum-dot cellular automata devices.
- Giovanna Turvani** received the M.Sc. degree in Electronics Engineering in 2012 and the Ph.D. degree from the Politecnico di Torino. She was Postdoctoral Research Associate at the Technical University of Munich in 2016. She is currently Postdoctoral Research Associate at Politecnico di Torino. Her interests include CAD Tools development for non-CMOS nanocomputing, architectural design for FCN and high-level device modeling. She is currently involved in a national project on microwave imaging technology for brain stroke monitoring.
- Gianluca Piccinini** received the Dr. Eng. and Ph.D. degrees in electronics engineering, in 1986 and 1990, respectively. Since 2006, he is Full Professor at the Department of Electronics, Politecnico di Torino and since 2016 is Lecturer at Electrical Engineering EPFL EDEE-ENS in Lausanne. His current interests include the introduction of new technologies in integrated systems, where he studies transport and advanced fabrication for molecular scale systems.
- Mariagrazia Graziano** received the Dr. Eng. and the Ph.D. degrees in Electronics Engineering from the Politecnico di Torino, in 1997 and 2001, respectively. Since 2002, she has been with the Politecnico di Torino as a Researcher and since 2005, as an assistant professor. Since 2008, she is Adjunct Faculty at the University of Illinois at Chicago (UFL), Chicago, and from 2014 to 2017 a Marie-Sklodowska-Curie IntraEuropean Fellow at the London Centre for Nanotechnology and University College London. Since 2015 she is a Lecturer at the École Polytechnique Fédérale de Lausanne. Her research interests include the design of CMOS and “beyond CMOS” devices, circuits, and architectures for nanocomputing, Field Coupling Nanocomputing and Quantum Computing.